AFGL-TR-88-0195

Scientific Background and Design Specifications for a Near-Earth Heliospheric Imager

B. V. Jackson

University of California
Electrical Engineering and Computer Sciences
San Diego, CA

9 August 1988

Final Report
1 March 1985 - 30 September 1987

Air Force Geophysics Laboratory
Air Force Systems Command
United States Air Force
Hanscom AFB, Massachusetts 01731

This technical report has been reviewed and is approved for publication.

RICHARD C. ALTROCK
Contract Manager

STEPHEN L. KEIL, Chief
Solar Research Branch

FOR THE COMMANDER

RITA C. SAGALYN, Director
Space Physics Division

This report has been reviewed by the ESD Public Affairs Office (PA), and is releasable to the National Technical Information Service (NTIS).

Qualified requestors may obtain additional copies from the Defense Technical Information Center. All others should apply to the National Technical Information Service.

If your address has changed, or if you wish to be removed from the mailing list, or if the addressee is no longer employed by your organization, please notify AFGL/DAA, Hanscom AFB, MA 01731. This will assist us in maintaining a current mailing list.

Do not return copies of this report unless contractual obligations or notices on a specific document requires that it be returned.

SECURITY CLASSIFICATION OF THIS PAGE

REPORT DOCUMENTATION PAGE

Form Approved
OMB No. 0704-0188

1a. REPORT SECURITY CLASSIFICATION Unclassified	1b. RESTRICTIVE MARKINGS
2a. SECURITY CLASSIFICATION AUTHORITY	3. DISTRIBUTION/AVAILABILITY OF REPORT Approved for public release; distribution unlimited.
2b. DECLASSIFICATION/DOWNGRADING SCHEDULE	
4. PERFORMING ORGANIZATION REPORT NUMBER(S)	5. MONITORING ORGANIZATION REPORT NUMBER(S) AFGL-TR-88-0195
6a. NAME OF PERFORMING ORGANIZATION University of California, San Diego 6b. OFFICE SYMBOL (If applicable)	7a. NAME OF MONITORING ORGANIZATION Air Force Geophysics Laboratory
6c. ADDRESS (City, State, and ZIP Code) Electrical Engineering & Computer Sciences La Jolla CA 92093	7b. ADDRESS (City, State, and ZIP Code) Hanscom AFB Massachusetts 01731-5000
8a. NAME OF FUNDING/SPONSORING ORGANIZATION 8b. OFFICE SYMBOL (If applicable)	9. PROCUREMENT INSTRUMENT IDENTIFICATION NUMBER F19628-85-K-0037
8c. ADDRESS (City, State, and ZIP Code)	10. SOURCE OF FUNDING NUMBERS PROGRAM ELEMENT NO. 61102F; PROJECT NO. 2311; TASK NO G3; WORK UNIT ACCESSION NO. DD

11. TITLE (Include Security Classification)
Scientific Background and Design Specifications for a Near-Earth Heliospheric Imager

12. PERSONAL AUTHOR(S)
B. V. Jackson

13a. TYPE OF REPORT	13b. TIME COVERED	14. DATE OF REPORT (Year, Month, Day)	15. PAGE COUNT
Final	FROM 3/1/85 TO 9/30/87	1988 August 9	18

16. SUPPLEMENTARY NOTATION

17. COSATI CODES			18. SUBJECT TERMS (Continue on reverse if necessary and identify by block number)
FIELD	GROUP	SUB-GROUP	Interplanetary Space, Coronal Physics, Solar Wind

19. ABSTRACT (Continue on reverse if necessary and identify by block number)

This report is intended to define the instrument specifications for a heliospheric imager capable of observing transient, diffuse features in the heliosphere from a spacecraft near 1 AU. These features include coronal mass ejections, co-rotating density enhancements, shock waves and any other disturbances that can affect the intensity of the electron-scattering coronal brightness. Our technique of imaging a large portion of the heliosphere using the HELIOS spacecraft zodiacal-light photometers has shown that it is possible to measure the structures around a spacecraft and to make good measurements of material in and out of the ecliptic plane. The HELIOS data show that it is possible to determine the velocities and spatial distributions of the large-scale features which propagate into the heliosphere.

(continued on reverse side)

20. DISTRIBUTION/AVAILABILITY OF ABSTRACT ☐ UNCLASSIFIED/UNLIMITED ☐ SAME AS RPT. ☐ DTIC USERS	21. ABSTRACT SECURITY CLASSIFICATION Unclassified
22a. NAME OF RESPONSIBLE INDIVIDUAL Richard C. Altrock	22b. TELEPHONE (Include Area Code) 22c. OFFICE SYMBOL AFGL/PHS

DD Form 1473, JUN 86 *Previous editions are obsolete.*

The instrumentation may be regarded as a successor to the zodiacal-light photometers of the HELIOS spacecraft. Such a second-generation instrument based on these principals could make effective use of *in situ* solar wind data from spacecraft in the vicinity of the imager, and would allow study of the effects of heliospheric structure interaction with the magnetosphere as never before possible. In addition, the imager would allow up to three days warning of the arrival of a mass ejection at Earth from the Sun.

1. Introduction

The measurement of diffuse sky brightness has progressed slowly over the years motivated largely by a desire to study the zodiacal dust cloud. The HELIOS photometric system (see section 2 below) has produced the most interesting results: although it failed to detect time variations in the zodiacal cloud itself, it succeeded well in detecting transient phenomena due to "plasma" effects, i.e. ordinary coronal electron-scattered continuum (Richter et al., 1982). The transient phenomena studied thus far have included coronal mass ejections (Jackson and Leinert, 1985; Jackson, 1985d), co-rotating features (Jackson, 1985c; 1989), shocks (Jackson, 1986) and comets (Benensohn and Jackson, 1987).

The HELIOS data showed that the intensity of Thomson-scattered light in the outer corona is great enough so that the entire heliosphere, at least in terms of variable structure out to 1 AU, can be remotely sensed by suitable photometric systems. Such global observations provide the best possible input into efforts to model and understand the physics of heliospheric dynamics, and they provide the best possible data base upon which to forecast terrestrial effects of heliospheric disturbances. In addition, they also show that background light sources such as stars and the zodiacal light do not vary enough to confuse the faint electron Thomson-scattering signal at distances from the Sun of 1 AU.

We use the HELIOS data and other calculations of brightness from expected heliospheric structures to define the signals present from these structures at 1 AU (Section 2). These determine the instrument specifications for a heliospheric imager specifically optimized to study these disturbances from a spacecraft near 1 AU. Section 3 summarizes the design considerations necessary to obtain observations and a monitoring capability from such a spacecraft. In section 4, the scientific and monitoring objectives of an imager situated near Earth are summarized. We feel that there is enormous potential in a new series of optimized observations for understanding the dynamics of the heliosphere and the mechanisms that perturb the solar-terrestrial environment.

2.1 Scientific Background - Features Observed By HELIOS

The two HELIOS spacecraft, of which the first was launched into heliocentric orbit in 1974, contained sensitive zodiacal light photometers that imaged the sky from 0.3 to 1.0 AU (Leinert et al., 1981). Other sensitive zodiacal light photometers have been placed on PIONEER spacecraft and have measured brightness from beyond 1 AU (Weinberg, 1985). Leinert and his group showed that the HELIOS photometry was stable with time over several years, and could be calibrated to about 5%. They found that the zodiacal light itself was unchanging at this level, and published tables and formulae to describe its appearance quantitatively from the HELIOS orbit. Each of the HELIOS spacecraft contained three photometers for the study of the zodiacal light distribution (Leinert et al., 1981). These photometers, at 16°, 31° and 90° ecliptic latitude, sweep the celestial sphere to obtain data fixed with respect to the solar direction. The photometers scan through different color and polarizing filters to produce additional diagnostic information with a sample interval of about five hours. The HELIOS photometers observed many coronal mass ejections (Richter et al., 1982; Jackson, 1985b) and thus constitute a unique data base that provides views of coronal transient phenomena. Because the HELIOS orbit is free of Earth, these data combined with coronal data obtained from Earth provide a unique stereoscopic view of an entire hemisphere of the outer corona. This stereoscopic capability

has been a major objective of the International Solar Polar Mission and of several other proposed deep-space probes, but some of the desired capability exists in these serendipitous HELIOS data.

The HELIOS photometer data is available on computer tapes at the National Space Science Data Center. The image processing system we have developed to access these data has been demonstrated by constructing images of the interplanetary medium in motion picture form from several 2-month sequences of data; these data, and additional images of specific events, have been used to trace the time history of a variety of density enhancements. These observations, better than any others, show the information that could be expected from a heliospheric monitoring instrument placed at 1 AU near Earth.

A major achievement of past research at the University of California at San Diego has been measurement of interplanetary masses and speeds of coronal mass ejections also observed by coronagraphs, interplanetary scintillation measurements, and from *in situ* spacecraft measurements. The 2-D imaging technique which displays HELIOS data has been developed at UCSD. The combination of these data with others to provide stereoscopic views of coronal mass ejections has been used to advantage for each ejection studied. These studies form the basis of the papers (Jackson, 1985a; Jackson et al., 1985; and Jackson and Leinert, 1985; as reviewed in Jackson, 1985d).

The masses obtained from these observations indicate that indeed the material of a mass ejection observed in the lower corona continues to move outward into the interplanetary medium. Mass estimates of coronal mass ejections observed by HELIOS are generally approximately twice those determined by the SOLWIND coronagraph for the same events. This comparison is satisfactory given the measurement errors of both instruments, but it is consistent from ejection to ejection. We interpret the difference, if it is real, as due primarily to the inability of coronagraph images to measure the total mass of an ejection at any given instant in time (e.g. see Jackson, 1985d). The analyses of specific events show that coronal mass ejections supply significant mass to the interplanetary medium, and that the mass flow often extends over times longer than one day.

The shapes of three loop-like mass ejections observed by coronagraphs have been measured as they moved past the HELIOS photometers in order to determine their edge-on thicknesses. Jackson et al. (1985) find an extent in HELIOS data for each event studied that is nearly the same as in the coronagraph view. In yet another analysis of a mass ejection on May 7, 1979, Jackson et al. (1988a) trace a mass ejection to over 0.5 AU from the Sun and determine its detailed three-dimensional shape from the perspective views of SOLWIND and HELIOS. Ejection mechanisms which indicate that a loop-like coronal mass ejection is propelled outward by a loop current system (Anzer, 1978; Muschovias and Poland, 1978) do not fit the picture observed from the perspective views of the mass ejections. Either the ejection encounters additional forces other than the current propelling it outward, or the model is wrong. The possibility of continuous structural evolution as the ejection moves outward from the Sun can not be ruled out, and would be very interesting to determine by detailed observations.

One coronal mass ejection in particular (that of May 21, 1980) has been studied in detail as to its surface manifestation (McCabe et al., 1986). The perspective view from the HELIOS spacecraft combined with that for SOLWIND allows a far more accurate mass to be determined for this event. It also indicates a highly non-radial motion at the onset of the ejection. Thus, from this example it is clear that knowing the site of the ejection on

the solar surface does not necessarily imply good knowledge of the direction of travel of the major portion of ejected mass. Figures 1 and 2 give examples of one coronal mass ejection well-observed by HELIOS B. In the figures, the ejection can be seen to move outward from the Sun at approximately 500 km/s. Views looking away from the Sun show that the mass ejection engulfs the spacecraft and can be observed to move beyond it primarily to the solar northwest.

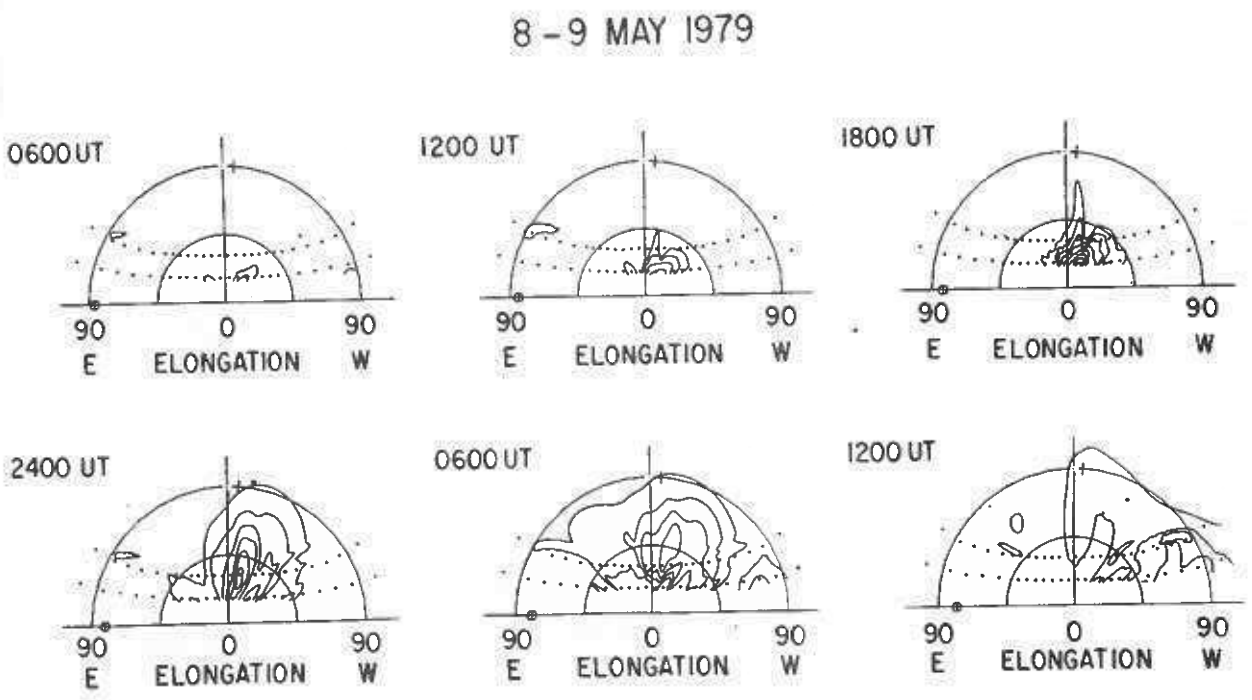

Fig. 1. HELIOS contour plots for the 7 May 1979 ejection as it moves outward from the Sun over a period from 0600 UT 08 May to 1200 UT 09 May. In this presentation, the Sun is centered and various solar elongations labeled on the abscissa form semi-circles above the ecliptic plane (represented by the horizontal line). The vertical line is the great circle to the north of the spacecraft. The position of the Earth is marked as the $\oplus$ near east 90° and the solar north pole tilt indicated by the short line segment crossing 90° elongation. Positions of the sector centers are marked by dots. Electron columnar density is contoured in levels of 3 $\times 10^{14} \mathrm{cm}^{-2}$. The larger elongations are generally the lowest level contoured.

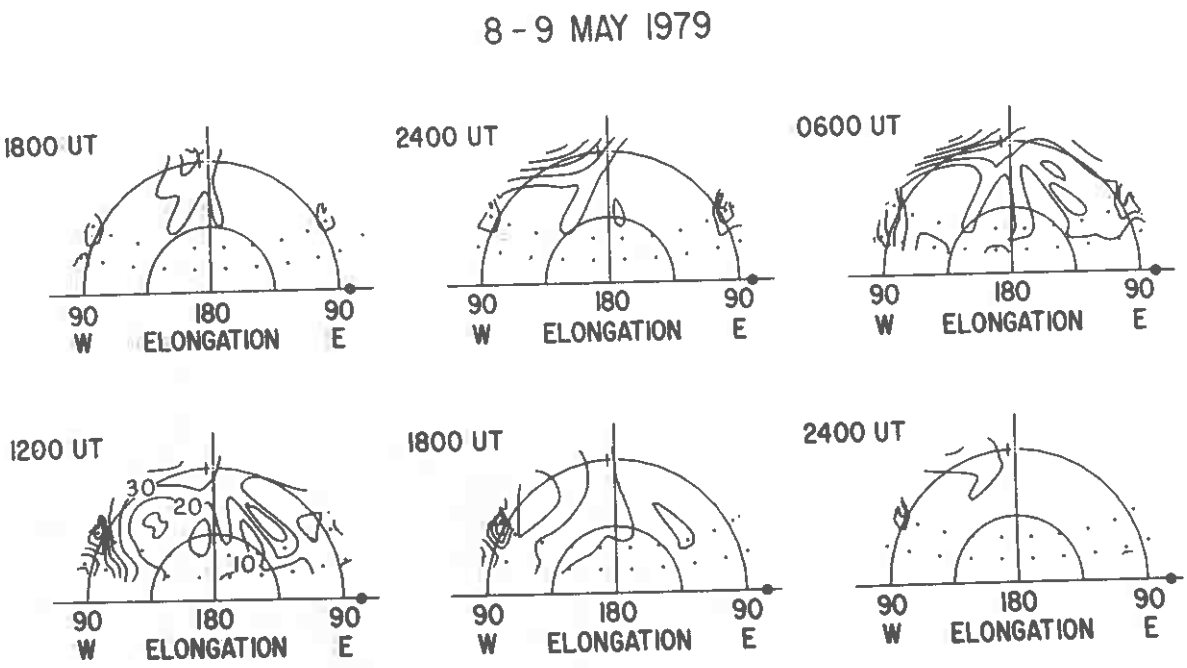

Fig. 2. HELIOS B contour plot for the 7 May 1979 ejection. In this presentation the direction 180° opposite the Sun is centered. Electron columnar density is contoured in levels of 10^{14}cm^{-2}. At 12:00 UT, contour levels are numbered.

The images have also been used to measure the extent of co-rotating density enhancements in the interplanetary medium. Figure 3 shows one such feature that can be followed for several days in HELIOS data. Measurement of the position angle motion of these features gives their heliospheric latitude and longitude. Measurement of their curvature with distance from the Sun gives a material speed (Jackson, 1985c). Careful analysis of more than thirty of the brightest and most distinct of these co-rotating features observed during several two-month intervals from 1976 to 1979 is currently underway (Jackson, 1989). The data show that these features generally outline magnetic field reversals near the solar surface (sector boundaries) during 1979 (Figure 4). They also indicate material speeds to 10% accuracy of approximately 300 km/s during 1979 up to 40° north latitude. At optimal times, the HELIOS photometers show these features to the east of the Sun prior to their arrival at the vicinity of the spacecraft. Thus, if operated in real time a near-Earth imaging system should be able to forecast the arrival of the sector boundary and co-rotating density enhancements.

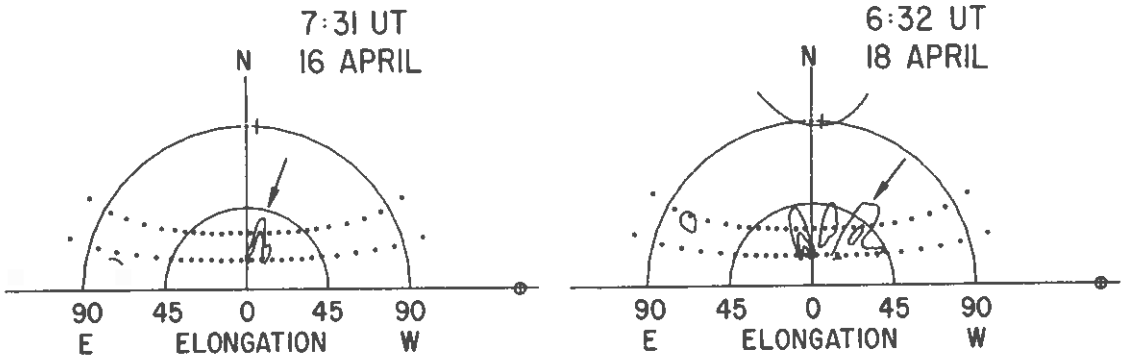

Fig. 3. HELIOS B contour plots showing a heliospheric co-rotating density enhancement (arrows mark the feature). In this presentation the Sun is centered. Electron columnar density is contoured in levels of 3 $\times 10^{14}$cm^{-2} upward from that level. The contours are drawn at times (given) when the 31° photometers measure brightness. Data from the 15° and 90° photometers are interpolated to the times indicated. (a and b) Movement of the feature from east to west over a period of approximately two days from April 16 to April 18, 1979.

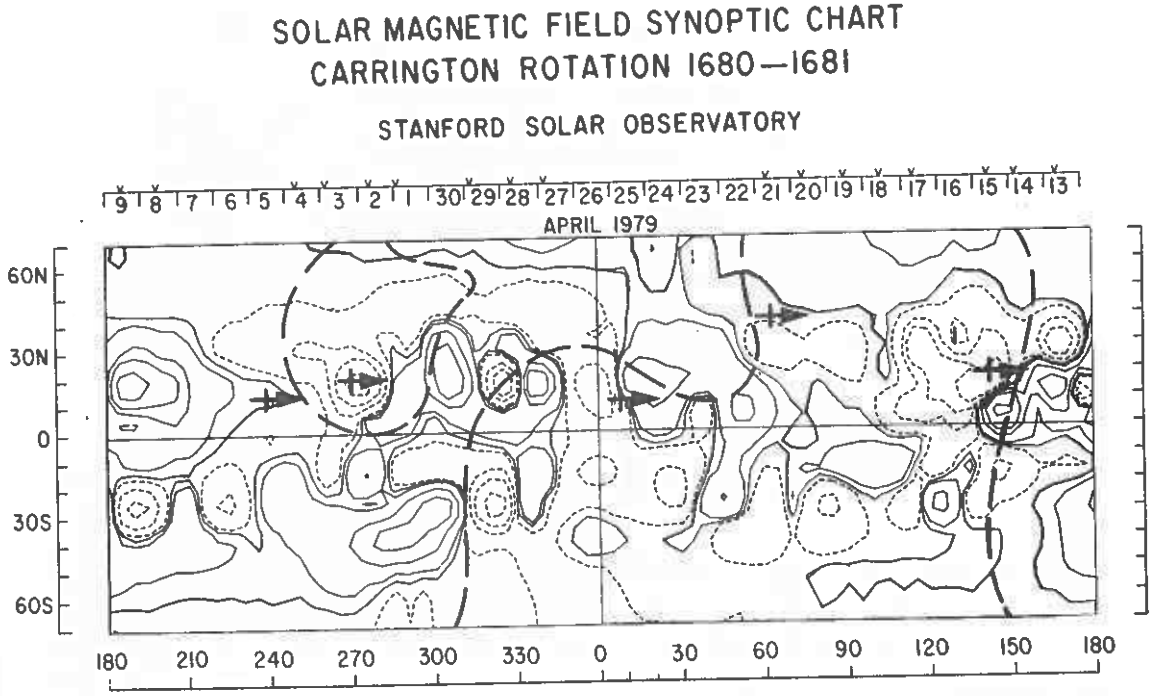

Fig. 4. Composite of two solar synoptic magnetic field maps (rotation 1680 and 1681) as in *Solar Geophysical Data*. Bold dashes mark potential field model sector boundaries at 2.6 R_s as in Hoeksema et al. (1983). Surface positions of five co-rotating features measured by HELIOS B are marked "→" assuming a constant velocity radial expansion.

The observations of these features from a heliospheric imager would thus provide a unique probe of interplanetary wind speed in and out of the ecliptic plane. The features are seen approximately at the brightness level expected from the ambient medium. The densities indicated are thus many times the ambient even for the high-latitude features. Notably, the density modeling of these features shows a difference in density above the ambient with height from the Sun. This difference observed along the height of the feature corresponds to fluctuations at a given height of a few days duration. At interplanetary distances these features can look similar to coronal mass ejections of small position angle extent.

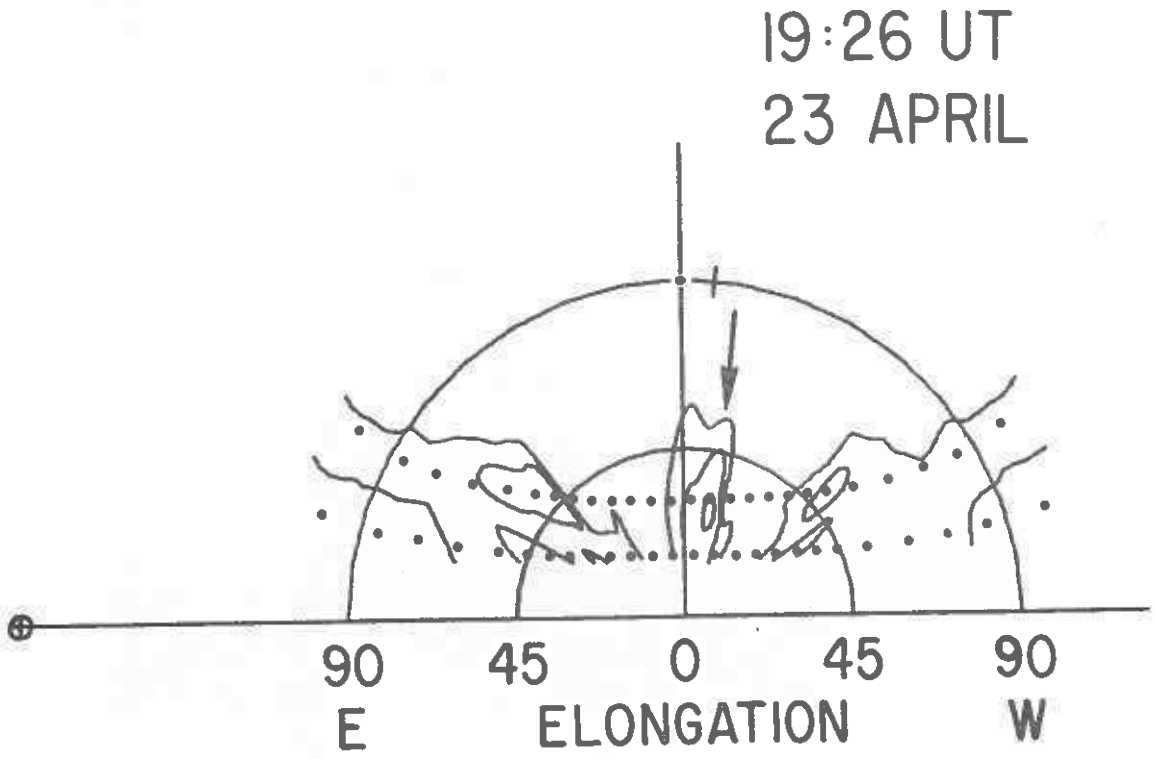

Fig. 5. HELIOS B photometer view of the density enhancement behind a shock also observed *in situ* by the spacecraft plasma probes. Electron columnar density is contoured in levels of 3 $\times 10^{14}\mathrm{cm}^{-2}$ upward from that level. The columnar density contours to either side of the spacecraft at 0.4 AU ($\geq$ 45° elongation) show the brightness from the enhanced density behind the shock front. The primary structure (arrow) is a heliospheric co-rotating feature, in this case, the extension of a coronal streamer and is not involved with the shock. The shock density enhancement lasts only a few hours in the plasma data. The brightness increase is registered on only one set of photometer observations, but because of the cadence (16° photometer, then 31° photometer) is observed at slightly lesser elongations in the 16° photometer. The enhancement can be observed sweeping past the spacecraft in the three-color cadence observed by the 31° photometer.

The density jump behind an interplanetary shock can manifest itself as a brightness increase in the HELIOS zodiacal light photometers. The shorter duration of these density increases challenges the capability of the 5-hour time cadence of the HELIOS photometer system. To help circumvent this problem we have developed an analysis program that uses the ten-minute time-cadence samples from a given photometer on HELIOS. To date we have measured five density enhancements behind shocks observed *in situ* (Jackson, 1986). While no three-photometer image capability exists for the brightness increases observed in the ten-minute cadence, there is enough information to map the general east-west extent of the shock front (to determine how the density enhancement relates to the magnetic shock normal). In some of the events it is also possible to observe the shock a few hours before it arrives at the HELIOS spacecraft. Radio observations and *in situ* density measurements, as well as brightness increases observed by HELIOS, indicate that interplanetary shocks are fairly extensive heliospheric features. In addition to mapping the extent of the interplanetary density increases behind shocks, we have attempted to use the UBV photometry on HELIOS to determine to what extent (if any) entrained dust plays a role in the outward moving shock. Figure 5 gives a blurred view of one of these shocks to either side (at 90° elongation) of the HELIOS spacecraft.

2.2 Scientific Background - Signal Levels Expected at 1 AU

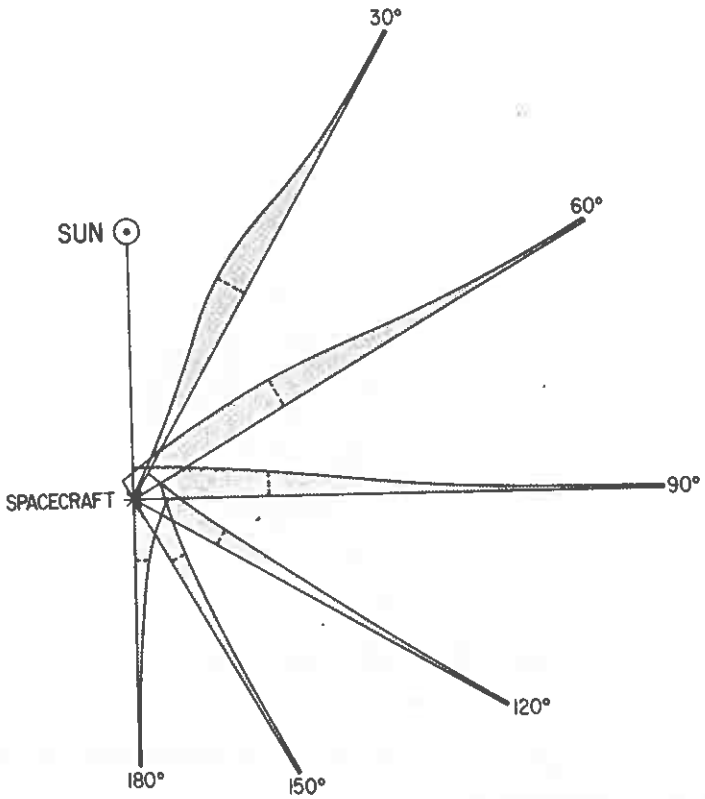

Fig. 6. Brightness contributions along the line of sight to the HELIOS photometer, as a function of elongation at 1.0 AU, for the Allen (1973) model corona. The dashed lines give the positions at which the integrated brightness reaches half of its total value.

By deliberately producing a heliospheric imager instrument optimized for the study of variable phenomena in the heliosphere, we could hope to gain a large factor of improvement over the HELIOS photometer design. The HELIOS photometers used classical design concepts and achieved great success, and it may be difficult to improve their photometric performance in a given angular sector. What we can certainly improve, however, is the angular and temporal sampling of the photometry. The HELIOS photometers scanned only a small fraction of the sky and in a heavily multiplexed fashion: successive samples were five hours apart. This was dictated in part by the 1 bit/second bit rate.

We would like to build a spacecraft instrument at least capable of observing coronal mass ejections at large solar elongations from near 1 AU. The brightnesses of the signal from coronal mass ejections can be estimated from Thomson scattering theory. In addition, we have a good idea of how visible these mass ejections will be above the ambient since the HELIOS spacecraft photometers have been used to trace coronal mass ejections observed near the solar surface by coronagraph techniques to nearly 1 AU distances from the Sun. Thomson electron scattering gives an estimate of the contribution to the brightness signal by the line-of-sight electron content in the ambient corona as shown in Figure 6. The total contribution of the integrated brightness signal with elongation is given in Figure 7.

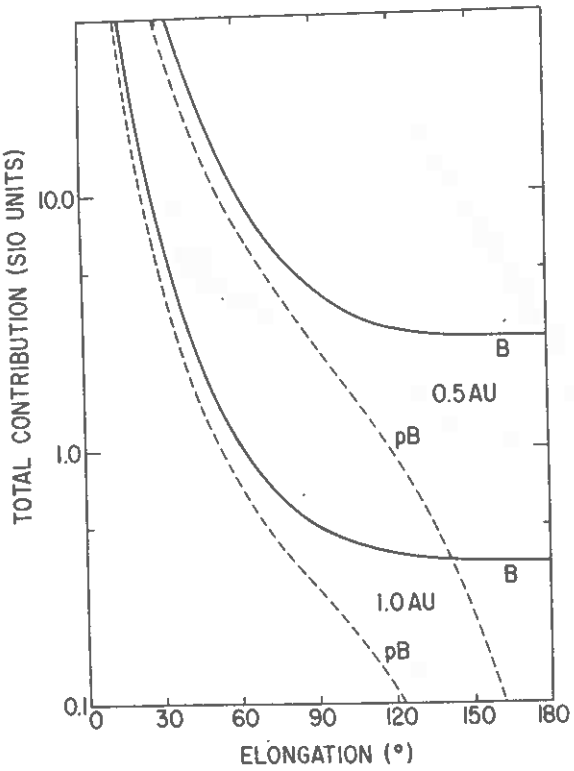

Fig. 7. Total integrated brightness at the HELIOS spacecraft vs. solar elongation for two spacecraft distances, 0.5 AU and 1.0 AU.

We have based this estimate upon the Allen (1973) model. Although a steady electron density such as the Allen corona would be very difficult to observe, it serves as a theoretical standard for the varying heliospheric excess densities we wish to measure. The heliospheric Allen corona decreases in density essentially as r^{-2} implying constant outward material

velocity. If a density excess such as a coronal mass ejection does not disperse as it moves outward, this excess density would be generally expected to retain its brightness level above the ambient. With this in mind, we have plotted the theoretical Allen corona and actual brightnesses of excess density features observed from the HELIOS spacecraft across its range of solar distances from 0.3 to 1.0 AU. This allows extrapolation to 1 AU distances where the HELIOS data are sparse. Figures 8 and 9a and b give the total integrated brightness from the model corona with spacecraft distance from the Sun for various elongations.

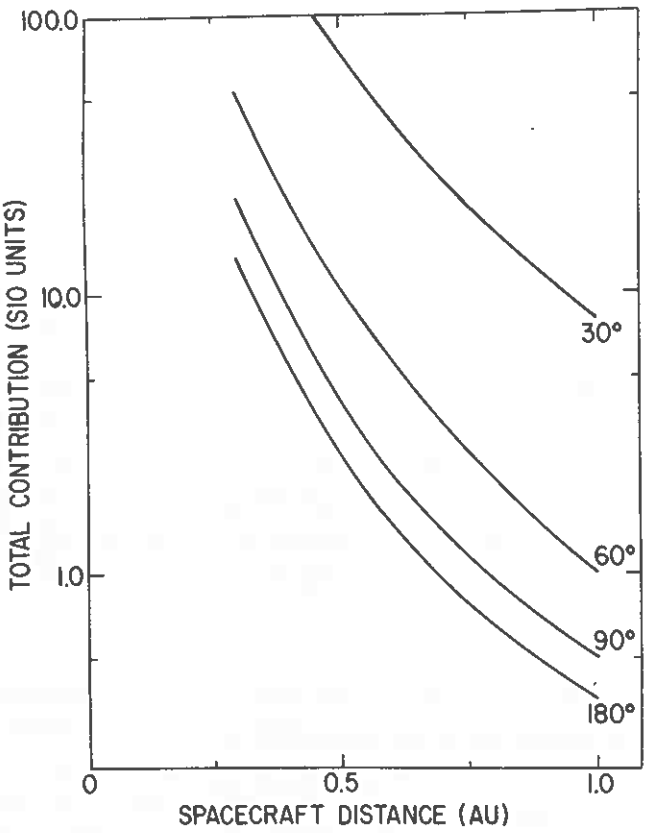

Fig. 8. Total integrated brightness at the HELIOS spacecraft vs. solar distance, for elongations of 30°, 60°, 90° and 180°.

The HELIOS B 16° photometer has been used to measure the 90° elongation rms amplitude of background fluctuations of duration less than four days over more than one spacecraft orbit, from April 4 to December 31, 1976. We plot these rms amplitudes in Figure 9. To first order, these variations decrease with radial distance similarly to the model coronal background, and from this we can estimate the approximate brightnesses of coronal structures near 1.0 AU. In general we find that the rms signal at 90° elongation has approximately the same magnitude as the model background (about 1.0 S10 unit). The starlight and stray light fluctuations must be kept to a few tenths of an S10 unit (0.1 S10 unit is the equivalent of one 12.5 mag star per square degree) over the several-day time interval of structure passage; this level was maintained on the average by the HELIOS B 16° photometer.

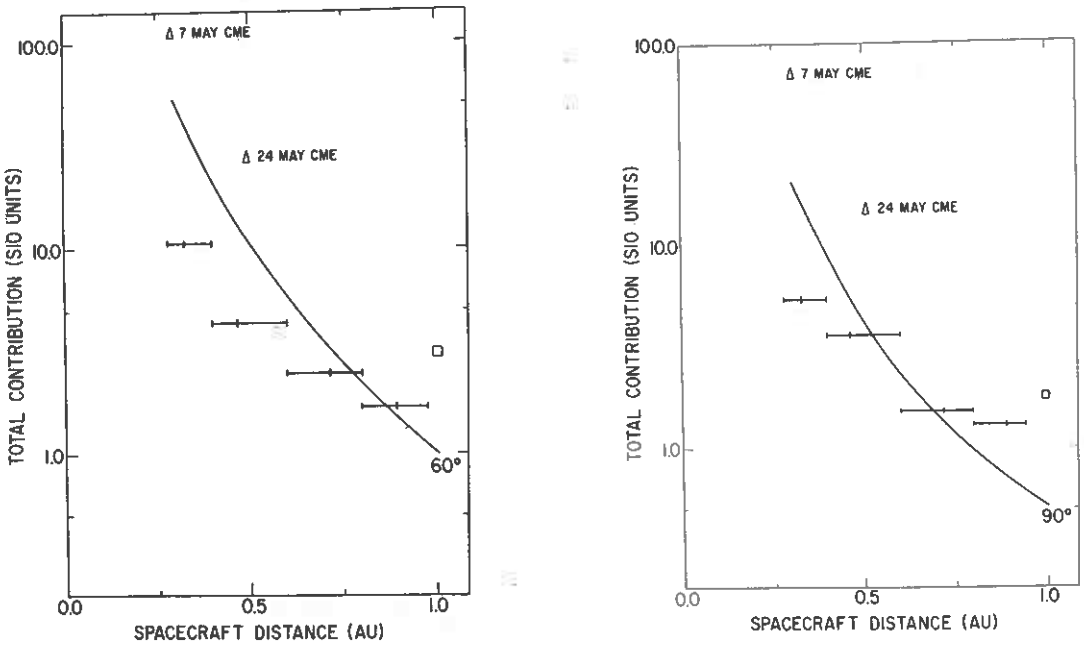

Fig. 9. Total integrated brightness at the HELIOS spacecraft vs. solar distance (smooth line). The histogram gives the rms amplitude of background brightness fluctuations. Average observed excess brightnesses of several coronal mass ejections traced outwards from SOLWIND coronagraph images are given as triangles, at the elongations observed by the HELIOS photometers. The square at 1.0 AU is the calculated signal from a typical large density increase observed *in situ*. a) 60° elongation; b) 90° elongation.

Figure 9 also shows the excess brightness of several coronal mass ejections at the elongations given; these ejections are shown to move outwards from SOLWIND coronagraph images. Were these ejections to move outward at constant speed without contracting or expanding, their brightnesses would remain in a constant ratio to the background. Finally, Figure 9 also shows the brightness expected from an *in situ* density of 50 cm^{-3} obtained by assuming this increase in density to be as extensive along the line of sight as is indicated by the time of passage of the density excess past the spacecraft.

Due to the motion of the spacecraft around the Sun, the photometer sectors appear to drift across the fixed stars. Each star enters the succeeding sector when this motion carries it there. The initial reduction of the HELIOS data provided positions good to 0.1° for HELIOS B, based upon checking against known positions of the bright stars (Leinert et al., 1981). In theory, this pointing accuracy should permit removal of stars down to 10th magnitude, given the average distribution of stars in the photometer field of view.

Other heliospheric phenomena that have been studied by HELIOS include comets and the solar cycle variability of mass ejections and the ambient medium. A more complete review of these observations can be found in Jackson (1988), Webb and Jackson (1987), and Leinert et al. (1989). There are many complex observational factors that will influence the design of an instrument built specifically to be operated near 1 AU. We are indeed fortunate that the HELIOS photometric data exists and can provide solid information as a starting point. Some of these considerations are discussed in the following paragraphs.

3. Design Considerations for a Heliospheric Imager

Signals to be Observed

Following the experience with the HELIOS spacecraft photometers, we have a good idea of the signal levels that can be expected from a variety of heliospheric features. Table 1 summarizes the signal levels described in the preceeding sections.

Table 1. Signal levels expected at one A.U.

Feature	Elongation (degrees)	Signal (S10)	Signal Duration (days)
Bright CME	60	3	1.5
	90	2	1.5
Bright Streamer	60	2	1
	90	1	1
Bright Shock	90	1-2	0.5
Major *in-situ*	60	3	2
fluctuation	90	2	2
Comet Shock	20	3-10	.1

Not only are signal levels important in the detection of features, but also the size of features is important in our ability to detect them. We determine noise levels referenced to a specific pixel size. Clearly, a feature that extends over more than one pixel or a feature that has a characteristic shape related to a grouping of pixels could be far more easily observed than indicated by the signal to noise present in a single pixel. Solar mass ejections are generally large features extending over many pixels, but their fronts, used to determine the onset of mass ejections, are not. Shock waves, thought to extend outward from the more dense regions of mass ejections, may be fairly small in comparison to mass ejections. The density enhancements (and depletions) associated with large co-rotating features should extend over large areas of space, while detailed structures near the onset of these features may not.

Background Light Components.

The diffuse sky brightness consists of several components, whose relative contributions depend upon ecliptic and galactic angular coordinates and on the location of the observer. To study the transient phenomena in the heliosphere, we need to be able to understand the unwanted background components as accurately as possible. One concern for a plasma imager will be a possible variable component of the Gegenschein sometimes reported from Earth's surface (Hong et al., 1985), but not observed to any appreciable extent from HELIOS. Essentially, we would like to be able to subtract the background light components, and we can do this only to the extent that we can accurately map them.

Stellar Contributions.

The sky brightness is normally expressed in S10 units: the equivalent number of 10th-magnitude stars per square degree. At 1 AU, in the range of elongations envisioned for

the heliospheric imager, the brightness varies from a few to a few hundred S10 units. It is clear that in pixels of subtense one square degree, individual stars will often make major contributions to the signal. This has three possible implications: first, the contributions of the brighter stars must be individually determined if they are to be accurately subtracted; second, the time variability of an individual star or its wander in and out of a pixel due to instrument pointing error might influence the sky-brightness measurement; finally, scattered light from the brighter stars and their motion relative to the Sun and Earth could conceivably produce a variable component in the darker image pixels. A simulation of the noise caused by starlight and the implimentation of a possible starlight rejection scheme designed for the Solar Mass Ejection Imager (SMEI) proposed for the WIND Spacecraft can be found in Jackson et al. (1988b) or Nichols (1987). Stellar rejection schemes such as the one described for the WIND Spacecraft rely on the discrete nature of stars to aid in their recognition and removal by over-resolving them in individual pixels.

Angular Pixel Size.

Since the primary goal of the heliospheric imager must be to study diffuse structures, high angular resolution is not a first priority. However, high resolution can be instrumental in recognizing the background light sources such as stars. It is always a good experimental principle to over-resolve the measured parameter. Also, there is no reason to doubt that interesting heliospheric phenomena also have interesting fine structure; for instance the nature of the structures that produce the interplanetary scintillation phenomenon is not presently well understood.

Field of View.

The best possible scientific return would come from the largest possible field of view, ranging from elongations at the borders of coronagraph fields of view to 180° elongation (i.e., the anti-solar direction). This would allow a nearly continuous tracking of those features which propagate to 1 AU from the solar surface. Co-rotating structures which are measured *in situ* could be traced to their solar origins over the distance from Sun to Earth. A view of the anti-solar direction, especially from Earth orbit would allow precise measurements of the Gegenschein and views of the region of the Geotail of the Earth.

Time Resolution.

The transient phenomena in the corona have relatively long time scales, but given a shock wave with a speed 3000 km/s, one would estimate a crossing time of only 15 minutes for a one-degree pixel at 1 AU. We would therefore like to have a sampling time on this order or better. The time scales will decrease further for nearby objects or smaller pixel sizes. Data bit rates and optical light-gathering capability available from different spacecraft may dictate the data rates that it is possible to use. Photon statistics and the size of the imager lens system may further dictate the integration time necessary to obtain an image at large elongations. With unlimited data rates, almost no on board processing or image storage is a possibility. This could significantly decrease imager spacecraft instrument costs.

Pointing Accuracy.

The HELIOS measurements were made on a spin-stabilized platform, so we know that this approach will work when the pointing accuracy available was approximately 0.1 degree. A less accurate pointing capability would mean that it would be less easy to hold star brightnesses constant in any given pixel. A spacecraft capable of three-axis pointing control could be superior from the point of view of the control of background light sources, including light scattered from the spacecraft.

4. Scientific and Monitoring Objectives of an Heliospheric Imager and Conclusions.

Most of the objectives of a heliospheric imager placed at 1 AU have been shown feasible by the HELIOS spacecraft zodiacal light photometers. We wish to build a system to carry out the following objectives:

I. Science Objectives

A. Observe and measure coronal mass ejections as they propagate into the heliosphere from near the solar surface. Obtain motions, mass estimates, and relationships to heliospheric shocks for each mass ejection.

B. Measure interplanetary co-rotating density features to determine the position and density of structures near the heliospheric current sheet. Determine velocities by measurement of the Archimedean spiral. Determine stability of these structures with time.

C. Measure the extent of density increases behind heliospheric shocks as they form and propagate past the spacecraft. Determine the relationship of shocks to heliospheric mass ejections and to solar flares.

D. Determine extent and shape of density enhancements which are also observed *in situ* by Earth spacecraft plasma probes.

II. Monitoring Objectives

A. Monitor solar mass ejections and their outward motion towards Earth.

B. Monitor the position of the heliospheric current sheet and the density enhancements near it in order to forecast their arrival at Earth.

C. Monitor the progress of and forecast the arrival at Earth of heliospheric shocks in the vicinity of the imager.

The elongation angles observed by this instrument give it the ability to bridge the gap between coronagraph observations and heliospheric regions measured *in situ*. Operated in real time, we presume that this instrument could regularly monitor the Earth space environment and give several days warning of the heliospheric structures that interact with the magnetosphere of the Earth.

Acknowledgements

I appreciate many helpful discussions with my colleagues about these analyses, especially those with Ch. Leinert who has graciously supported the HELIOS data reduction, in part by his grant WRS-0108. Data from the HELIOS photometers is available at the National Space Science Data Center, Goddard, USA. In addition to Air Force Contract F19628-85-0037, the work described here was supported in part by National Science Foundation Grant ATM86-09469 to the University of California, San Diego.

References

1. Allen, C. W., *Astrophysical Quantities*, 3rd ed., p. 176, Athlone, London, 1973.

2. Anzer, U., "Can Coronal Loop Transients be Driven Magnetically?", *Solar Phys.*, **57**, 111, 1978.

3. Benensohn, R.M. and Jackson, B.V., "Comet West 1976 VI; A view from the Helios zodiacal light photometers", in Proc. STIP Symposium of Solar/Interplanetary and Cometary Intervals, 12-15 May, Huntsville, Alabama, USA, 1987.

4. Hoeksema, J. T., Wilcox, J. M., and Scherrer, P. H., "The Structure of the Heliospheric Current Sheet: 1978-1982", *J. Geophys. Res.*, **88**, 9910, 1983.

5. Hong, S. S., Misconi, N. V., van Dijk, M. H. H, Weinberg, J. L., and Toller, G. N., "A Search for Small Scale Structures in the Zodiacal Light", in proceedings of Properties and Interactions of Interplanetary Dust, Giese, R. H. and Lamy, P., eds., 33, 1985.

6. Jackson, B. V., "Helios Observations of the Earthward-Directed Mass Ejection of 27 November, 1979", *Solar Phys.*, **95**, 363, 1985a.

7. Jackson, B.V., "Review of STIP Interval VI: 15 April - 15 June 1979", to be published in *Proceedings of the STIP Symposium on Retrospective Analyses and Future Coordinated Intervals*, 10-12 June, Les Diablerets, Switzerland, 1985b.

8. Jackson, B.V., "Helios Observations of a Coronal Streamer During STIP Interval VI", to be published in *Proceedings of the STIP Symposium on Retrospective Analyses and Future Coordinated Intervals*, 10-12 June, Les Diablerets, Switzerland, 1985c.

9. Jackson, B. V., "Imaging of Coronal Mass Ejections by the Helios spacecraft", *Solar Phys.*, **100**, 563, 1985d.

10. Jackson, B.V., "Helios Photometer Measurement in In Situ Density Enhancements", *Adv. in Space Res.*, **6**, 307, 1986.

11. Jackson, B.V., "Heliospheric Remote Sensing Using the Zodiacal Light Photometers of the Helios Spacecraft", Yosemite 1988 Conference on Outstanding Problems in Solar System Plasma Physics: Theory and Instrumentation, Yosemite National Park, California, February 2-5, 1988, accepted for publication, June, 1988.

12. Jackson, B.V., "Helios Spacecraft Photometer Observations of Elongated Co-Rotating Structures in the Interplanetary Medium", in preparation to be submitted to the *J. Geophys. Res.*, 1989.

13. Jackson, B. V., Howard, R. A., Sheeley, Jr., N. R., Michels, D. J., Koomen, M. J., and Illing, R. M. E., "Helios Spacecraft and Earth Perspective Observations of Three Looplike Solar Mass Ejection Transients", *J. Geophys. Res.*, **90**, 5075, 1985.

14. Jackson, B. V., and Leinert, C., "Helios Images of Solar Mass Ejections", *J. Geophys. Res.*, **90**, 10759, 1985.

15. Jackson, B.V., Rompolt, B., and Svestka, Z., "Solar and Interplanetary Observations of the Mass Ejection on 7 May 1979", *Solar Phys.*, in press, 1988a.

16. Jackson, B.V., H.S. Hudson, J.D. Nichols and R.E. Gold, 'Design Considerations for a "Solar Mass Ejection Imager" on a Rotating Spacecraft', Yosemite 1988 Conference on Outstanding Problems in Solar System Plasma Physics: Theory and Instrumentation, Yosemite National Park, California, February 2-5, 1988, submitted March, 1988b.

17. Leinert, Ch., R. Schwenn and B.V. Jackson, "Variation of Solar Cycle Mass Flux - A Comparison of Helios Photometer In-Situ and IPS Data", in preparation to be submitted to the *J. Geophys. Res.*, 1989.

18. Leinert, C., Pitz, E., Link, H., and Salm, "Calibration and In-Flight Performance of the Zodiacal Light Experiment on Helios", *Space Sci. Instrum.*, **5**, 257, 1981.

19. McCabe, M. K., Svestka, Z. F., Howard, R. A., Jackson, B. V., and Sheeley, Jr., N. R., "Coronal Mass Ejection Associated with the Stationary Post-Flare Arch of 21/22 May 1980", *Solar Phys.*, **103**, 399, 1986.

20. Muschovias, T., and Poland, A. I., "Expansion and Broadening of Coronal Loop Transients: A Theoretical Explanation", *Astrophys. J.*, **110**, 115, 1978.

21. Nichols, J.D., "Data Simulations for a Rotating Heliospheric Imager", UCSD report SP-87-23, 1987.

22. Richter, I., Leinert, C., and Plane, B., "Search for Short Term Variations of Zodiacal Light and Optical Detection of Interplanetary Plasma Clouds", *Astron. Astrophys.*, **110**, 115, 1982.

23. Webb, D.F. and B.V. Jackson, "Detection of CME's in the Interplanetary Medium from 1976-1979 Using HELIOS-2 Photometer Data", in *Proc. of the 6th Solar Wind Conference*, 267, 1987.

24. Weinberg, J. L., "Zodiacal Light and Interplanetary Dust", in *Proc. of Properties and Interactions of Interplanetary Dust*, Giese, R. H. and Lamy, P., eds., 1, 1985.